Applied Mathematical Modelling 84 (2020) 106–115

Contents lists available at ScienceDirect

Applied Mathematical Modelling

journal homepage: www.elsevier.com/locate/apm

Average steady flow toward a drain through a randomly heterogeneous porous formation

Gerardo Severino[a,*], Carmine Fallico[b], Samuele De Bartolo[c]

[a] Department of Agricultural Sciences, University of Naples – Federico II, Italy
[b] Department of Civil Engineering, University of Calabria, Italy
[c] Department of Engineering for Innovation, University of Salento, Italy

ARTICLE INFO

Article history:
Received 9 March 2019
Revised 25 March 2020
Accepted 30 March 2020
Available online 9 April 2020

Keywords:
Porous media
Steady flow
Drain
Heterogeneity
Stochastic modelling
Equivalent conductivity

ABSTRACT

We consider the problem of steady pumping of water from a line drain on the surface of a wet ground. Unlike the classical formulation, which regards the conductivity parameter K as uniformly distributed in the domain, the problem here is solved within a stochastic framework in order to account for the irregular (random), and more realistic, spatial variability of K. Due to the linearity of the problem at stake, we focus on the derivation of the mean Green function G. This is computed by means of an asymptotic expansion.

The fundamental result is an analytical (closed form) expression of G which generalizes the classical solution. Based on this, we develop an equivalent conductivity K^{eq} which enables one to tackle the problem similarly to the classical one. In particular, it is shown that the equivalent conductivity grows monotonically with the radial distance r from the drain, and it lies within the range $K^{\mathrm{eq}}(0) \leq K^{\mathrm{eq}}(r) \leq K^{\mathrm{eq}}(\infty) < \infty$.

1. Introduction

Understanding of pattern of shallow water-tables due to drainage is crucial from an environmental and from an agricultural point of view. While the knowledge of the water-table regime may be sufficient to design drainage network(s) [see, e.g. 1], precise estimations of the flow pattern determined by a drain (or a battery of drains) are required to assess environmental impacts on hydrological regime and pollutant loads.

Typically, the available field data gives only information on the amount of water that flows along a drain, while the physical processes controlling water floware hardly measurable. Nevertheless, extra monitoring devices would result excessively expensive. Within such a view, mathematical modelling of a drain-type flow lends itself as a necessary tool to characterize flow around a line of drainage. Several models have been developed to simulate drainage processes [see, e.g. 2]. Depending on the specific simulation needs, models have focused on simulating hydrological processes at different scales [a comprehensive review can be found in 3, and references therein]. Common to all classical analytical studies is regarding as a constant the conductivity K of the constitutive (Darcy's) law

$$\mathbf{q}(\boldsymbol{x}) = -K\nabla h(\boldsymbol{x}), \tag{1}$$

* Corresponding author at: Department of Agricultural Sciences, University of Naples – Federico II - Division of Water Resources Management and Biosystems Engineering via Universit 100, Portici (Naples) I80055, Italy.

E-mail address: gerardo.severino@unina.it (G. Severino).

https://doi.org/10.1016/j.apm.2020.03.038

relating the flux $\mathbf{q}$ [L/T] to the gradient of the hydraulic head (energy per unit weight) h [L]. However, geological formations are *de facto* heterogeneous with K varying in the space quite largely [see, e.g. the data survey in 4]. These irregular changes have a tremendous impact upon flow (and transport) taking place in porous formations [5]. The common (and widely accepted) approach to tackle these erratic spatial variations is a stochastic framework [4–6]. In principle, this approach recognizes that the conductivity is affected by uncertainty [see, e.g. the field findings in 7,8], and regards it as a *random space function* (RSF). This state of affair renders stochastic the flow equation, and therefore predictions are made in terms of probabilities rather than in the traditional (deterministic) framework [9]. Since in the applications one is interested into the spatial average $\overline{h}$ of the hydraulic head, it is assumed that the space domain over which such an average is computed is large enough as compared with the heterogeneity correlation scale(s) of K, so that one can exchange the spatial average with the ensemble average (ergodicity), i.e. $\overline{h} \simeq \langle h \rangle$. We shall follow the same avenue in the present study.

The central problem of modelling flow through spatially heterogeneous porous formations can be formulated as follows: given the domain $\Omega \subseteq \mathbb{R}^3$ and the boundary conditions on $\partial\Omega$, determine the mean head $\langle h \rangle$. This problem is similar to many others encountered in *Physics* and *Engineering* [see, e.g. 10,11]. The resulting stochastic flow-equation(s) can be solved either analytically or numerically by *Monte Carlo simulations* (MCs). These latter are conceptually simple and applicable to a large variety of boundary conditions. However, MCs pose a number of serious drawbacks and limitations. Indeed, to account for high-frequency fluctuations of the input RSFs, very fine numerical grids are required. As a consequence, each realization may result computer-demanding, especially when one deals with three-dimensional flows. In addition, even if MCs converge after a sufficiently large number of runs, there is not a systematic procedure to ascertain whether to consider conclusive, and therefore completed, MCs [a deep discussion upon these issues can be found in 12]. To the contrary, analytical results avoid the lack of accuracies attached to MCs [a wide survey can be found in 13, and references therein]. Analytical methods enable one to obtain (by ensemble averaging) deterministic equations which are solved for the mean values of the dependent flow variables. Not disregarded, analytical solutions serve as benchmark to validate numerical simulations. Finally, unlike MCs, analytical solutions also provide explicit relationship between the input parameters and the model output, therefore giving direct physical insight to the problem at stake.

In line with the standard practice [4], we assume that conductivity $K \equiv K(\boldsymbol{x})$ appearing into (1) is a second order stationary (statistically homogeneous) RSF with constant mean $\langle K \rangle$ and variance σ_K^2. Then, we introduce the zero mean RSF $\varepsilon(\boldsymbol{x}) = 1 - K(\boldsymbol{x})/\langle K \rangle$, and substitute into (1), to have

$$\mathbf{q}(\boldsymbol{x}) = -\langle K \rangle [1 - \varepsilon(\boldsymbol{x})] \nabla h(\boldsymbol{x}), \qquad \forall \boldsymbol{x} \in \Omega. \tag{2}$$

To compute $\langle h \rangle$, we supplement (2) with the mass conservation law, i.e. $\nabla \cdot \mathbf{q} = 0$. Hence, substituting (2) into the latter leads to the following Poisson-type stochastic equation:

$$\nabla^2 h(\boldsymbol{x}) = \nabla \cdot [\varepsilon(\boldsymbol{x}) \nabla h(\boldsymbol{x})], \qquad \forall \boldsymbol{x} \in \Omega \tag{3}$$

to be solved within the domain Ω, under the proper boundary condition(s).

Most of the previous studies were limited to the so called mean uniform flow, i.e. a flow with constant mean velocity that is determined by a constant head gradient on the boundary $\partial\Omega$ [see, e.g. 4,5, and references therein]. However, as stated above there are important real-world situations in which the mean uniform condition is not met. This is the typical case of source-type flows, the most ubiquitous ones being those of injecting/pumping wells and drains. In spite of their importance for the applications, these flows (that are characterized by a mean velocity that is not constant) have been studied to a lesser extent, mainly because of the mathematical complexity. While recently there have been remarkable results in the theory of wells [e.g. [14–16]], we are not aware about any advancement on the case of a flow toward a drain. The present study represents a first step on this topic.

The plan of the paper is the following: we consider a steady flow toward a drain located on the boundary of a wet ground, and we are interested into characterizing the flow-pattern as affected by the medium's heterogeneity. In particular, we aim at computing the mean head by means of the appropriate Green function G, which is constructed *ad hoc* along the lines traced by Indelman [17]. To our knowledge, such a problem has never been tackled by means of analytical tools (partly due to the mathematical difficulties). For a formation of isotropic heterogeneity structure, an analytical expression for G is derived. This enables one to investigate the flow toward a drain through the heterogeneous medium by computing in analytical form the mean head as: $\langle h \rangle = h_0 + \sigma^2 \langle h_2 \rangle$, being h_0 the homogeneous (no heterogeneity) head, whereas $\langle h_2 \rangle$ adjusts h_0 according to the heterogeneity. Finally, the concept of equivalent conductivity is employed in order to cast the problem at stake within the stand point of the theory of composites.

2. Mathematical statement and computation of the mean Green function

A semi-bounded domain (aquifer) $\Omega = \{\boldsymbol{x} \equiv (x_1, x_2, x_3) \in \mathbb{R}^3 : x_1 \leq 0\}$ is drained at a constant specific (i.e. per unit length of drain) discharge Q_w by a drain of length 2Δ located on the upper-boundary Ω (Fig. 1). The following assumptions are adopted in the present study. $\diamond$ The drain is modelled by a horizontal singular segment, i.e. $\delta(x_3)[\mathrm{H}(x_3 + \Delta) - \mathrm{H}(x_3 - \Delta)]$, being $\delta(x)$ and $\mathrm{H}(x)$ the Dirac distribution and the Heaviside step-function, respectively. The numerical error related to such an assumption is less than 4% if the radius r_d of the drain is lesser than $I/100$ [18], where $I \equiv \int_0^\infty \mathrm{d}r\, \rho(r)$ is the integral scale of the RSF ε. Since $I \simeq \mathcal{O}(\mathrm{m})$ [see, e.g. 4] and $r_d \simeq \mathcal{O}(\mathrm{cm})$, the above assumption is fulfilled in most of the practical

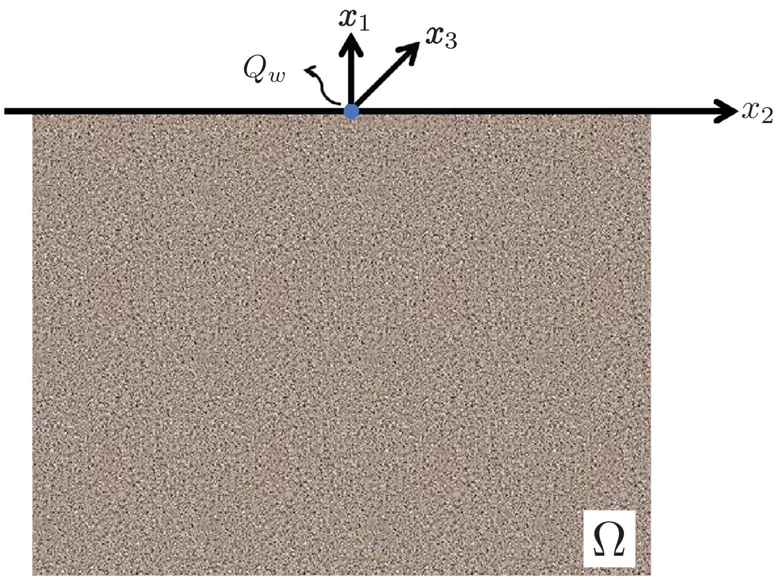

Fig. 1. Sketch of the flow domain Ω with a drain of constant specific volumetric rate Q_w, located at the upper boundary $x_1 = 0$.

situations. ◇ The non dimensional residual $\varepsilon(\boldsymbol{x}) = 1 - K(\boldsymbol{x})/\langle K\rangle$ is modeled as a stationary RSF of variance σ^2, and two-point autocorrelation $\rho(\boldsymbol{x}-\boldsymbol{y}) \equiv \langle\varepsilon(\boldsymbol{x})\varepsilon(\boldsymbol{y})\rangle$ (for any $\boldsymbol{x} \neq \boldsymbol{y}$). ◇ The ergodic hypothesis is obeyed if the length 2Δ of the drain is much larger than the integral scale I, i.e. $2\Delta \gg I$. This requirement supports the assumption of transversally unbounded domain and, at the same time, it authorizes to regard the drain as infinite. As such, hereafter we shall deal with the case $\Delta \to \infty$.

External boundary conditions for the stochastic equation (3) are determined by physical processes at the surface, and away from the drain. Let $\bar{\mathbf{q}} \equiv (\bar{q}_1, \bar{q}_2, \bar{q}_3)^\top$ denote the flux along the line-drain, from Darcy's law (1) it yields

$$\bar{q}_1 \equiv K_H \frac{\partial}{\partial x_1} h(\boldsymbol{x})\Big|_{x_1=0} = Q_w\,\delta(x_3), \tag{4}$$

being the conductivity along the drain localized by means of the harmonic mean, i.e. $K_H \equiv \langle K^{-1}\rangle^{-1}$ [for a deeper discussion, see 16,19]. Hence, (4) gives rise to a boundary condition:

$$\frac{\partial}{\partial x_1} h(\boldsymbol{x})\Big|_{x_1=0} = \bar{Q}_w\,\delta(x_3) \qquad -\infty < x_2,\ x_3 < +\infty \tag{5}$$

(with $\bar{Q}_w = Q_w/K_H$). Instead, far from the drain, one has

$$\lim_{r\to\infty} |\mathbf{q}(\boldsymbol{x})| = 0, \qquad r = \sqrt{x_1^2 + x_2^2}, \tag{6}$$

and therefore from the Darcy's law (1), the boundary condition reads as

$$\lim_{r\to\infty} \frac{\partial}{\partial r} h(\boldsymbol{x}) = 0, \qquad r = \sqrt{x_1^2 + x_2^2}. \tag{7}$$

Before proceeding further, we wish to clarify the physical significance of (5). In fact, to honor the mass conservation at the drain one has to require that, i.e.

$$Q_w = \int_\Omega \mathrm{d}\boldsymbol{x}\, e_m\, q_m(\boldsymbol{x}), \qquad m = 1, 2, \tag{8}$$

being $\mathbf{e} \equiv (e_1, e_2)^\top$ a unit vector. As a consequence, the flow at the surface results purely tangential in agreement with the boundary condition (5).

Due to the linearity of Eqs. (3) and (4), the mean head is calculated by the aid of the Green function G, i.e.,

$$\langle h(\boldsymbol{x})\rangle = \int_{\mathbb{R}^2} \mathrm{d}\boldsymbol{\xi}\, G\big(\boldsymbol{x}; \boldsymbol{\xi}\big) \frac{\partial}{\partial \xi_1} h\big(\boldsymbol{\xi}\big). \tag{9}$$

Most of the past literature on the subject referred to infinite domains [e.g. [17,20–22]]. Nevertheless, the construction of $G(\boldsymbol{x}; \boldsymbol{x}')$ for any bounded domain can be treated by the method of images in which the mean Green function, i.e.

$$G_\infty(\boldsymbol{x}) = G_\infty^{(0)}(x) + \sigma^2 G_\infty^{(2)}(\boldsymbol{x}) \tag{10}$$

$$G_{\infty}^{(2)}(\boldsymbol{x}) = \frac{1}{3}\,G_{\infty}^{(0)}(x) + \int d\bar{\boldsymbol{x}}\,\rho(\bar{\boldsymbol{x}})\,\frac{|\boldsymbol{x}-\bar{\boldsymbol{x}}|}{2\bar{x}}\left[\frac{3(\bar{x}^2-\boldsymbol{x}\cdot\bar{\boldsymbol{x}})^2}{\bar{x}^2(\boldsymbol{x}-\bar{\boldsymbol{x}})^2}-1\right]\frac{d}{d\bar{x}}G_{\infty}^{(0)}(\bar{x})\,\frac{d}{dy}G_{\infty}^{(0)}(y)\Big|_{y=|\boldsymbol{x}-\bar{\boldsymbol{x}}|} \tag{11}$$

[details are in 17] is reflected across $x_1 = 0$. The zero order term $G_{\infty}^{(0)}(x) = \frac{1}{4\pi x}$ is the Green function for a domain of constant conductivity $\langle K\rangle$. This leads to:

$$G(\boldsymbol{x};\boldsymbol{x}') = G_{\infty}(x_1 - x_1' + x_h) + G_{\infty}(x_1 + x_1' + x_h), \tag{12}$$

where $x_h = \sqrt{x_2^2 + x_3^2}$ is the magnitude of the vector $\boldsymbol{x}_h \equiv (x_2, x_3)$. For simplicity, we limit the present study to formations of isotropic heterogeneity structure, and we adopt exponential and Gaussian shape for the autocorrelation ρ, i.e.

$$\rho(x_1, x_h) = \begin{cases} \exp\left[-\sqrt{\left(\frac{x_1}{I}\right)^2 + \left(\frac{x_h}{I}\right)^2}\right] & \text{exponential} \\ \exp\left[-\frac{\pi}{4I^2}\left(x_1^2 + x_h^2\right)\right] & \text{Gaussian} \end{cases} \tag{13}$$

[see 4,5]. Thus, by employing the above described method of reflection, $G_{\infty}^{(2)}$ is expressed in closed analytical form as:

$$G_{\infty}^{(2)}(x) = \frac{1}{3}\,G_{\infty}^{(0)}(x) + \frac{\Lambda(x)}{24\pi} \tag{14}$$

$$\Lambda(x) = \begin{cases} \left(\frac{4}{\bar{x}} + 1 - \bar{x}\right)\exp(-\bar{x}) + \left(6 - \bar{x}^2\right)\mathrm{Ei}(-\bar{x}) & \text{exponential } \rho \\ \left(\frac{4}{\bar{x}} + \pi\bar{x}\right)\exp\left(-\pi\frac{\bar{x}^2}{4}\right) - \frac{\pi}{2}\left(6 + \pi\,\bar{x}^2\right)\mathrm{erfc}\left(\sqrt{\pi}\,\frac{\bar{x}}{2}\right) & \text{Gaussian } \rho \end{cases} \tag{15}$$

(with $\bar{x} = x/I$). Before going further, it is worth noting at this stage that for $\sigma^2 = 0$ one recovers results pertaining to a homogeneous (no heterogeneity). As a consequence, the mean Green function (12) can be regarded as a generalization of classical results. The contour-levels of the function G have been computed for $10^{-2} \le \frac{x_1}{I}, \frac{x_1'}{I} \le 10$, and they are depicted in the Fig. 2 for both exponential (continuous line) and Gaussian (dashed line) autocorrelation ρ. It is seen that the iso-values are symmetrically located with respect to the line $x_1 = x_1'$ (by virtue of the principle of symmetry). In addition, while the differences due to different shape of ρ are immaterial at distances greater than a few integral scales, they appear much more evident for $x_1/I, x_1'/I \le 0.1$.

Mean flow toward a drain

With the mean Green function previously determined, we are now in position to compute the mean head (9). At the σ^2-order of approximation it writes as

$$\langle h(\boldsymbol{x})\rangle = h_0(\boldsymbol{x}) + \sigma^2\langle h_2(\boldsymbol{x})\rangle. \tag{16}$$

The zero-order correction h_0, representing the solution pertaining to a homogeneous aquifer (i.e. $K \equiv \langle K\rangle\ \forall\boldsymbol{x} \in \Omega$), can be obtained by standards methods, and we limit to quote the final result $h_0(r) = -\frac{\bar{Q}_w}{\pi}\ln r$ [23,24]. The second order correction $\langle h_2\rangle$ is obtained from (9) as:

$$\langle h_2(r)\rangle = \frac{1}{3}\,h_0(r) + \frac{\bar{Q}_w}{3\pi}\,\omega(r), \qquad \omega(r) = \int_0^{\infty} d\xi\;\Lambda\left(\xi^2 + r^2\right), \tag{17}$$

where ω is computed (see the Appendix A for details) for exponential and Gaussian ρ, i.e.

$$\begin{aligned}\omega^{(\exp)}(r) = &-\ln\bar{r} + \left(\frac{\bar{r}}{3}\right)^2\mathrm{K}_2(\bar{r}) + \frac{2}{9}\bar{r}\left(\bar{r}^2 - 9\right)\mathrm{K}_1(\bar{r}) + \frac{1}{18}\left(4\bar{r}^4 - 45\bar{r}^2 + 36\right)\mathrm{K}_0(\bar{r}) \\ &+ \frac{\pi}{9}\bar{r}^2\left(\bar{r}^2 - 9\right)\left[\mathrm{K}_0(\bar{r})\mathrm{L}_1(\bar{r}) + \mathrm{K}_1(\bar{r})\mathrm{L}_0(\bar{r}) - \frac{1}{\bar{r}}\right],\end{aligned} \tag{18}$$

$$\omega^{(\mathrm{Gauss})}(r) = -\ln\bar{r} + \exp\left(-\frac{\pi}{8}\bar{r}^2\right)\left\{\frac{4+\pi\bar{r}^2}{16}\left[\left(4+\pi\bar{r}^2\right)\mathrm{K}_0\left(\frac{\pi}{8}\bar{r}^2\right) - \pi\bar{r}^2\mathrm{K}_1\left(\frac{\pi}{8}\bar{r}^2\right)\right] - \frac{\pi}{4}\bar{r}\mathrm{W}_{-1,1}\left(\frac{\pi}{4}\bar{r}^2\right)\right\} \qquad \bar{r} = \frac{r}{I}. \tag{19}$$

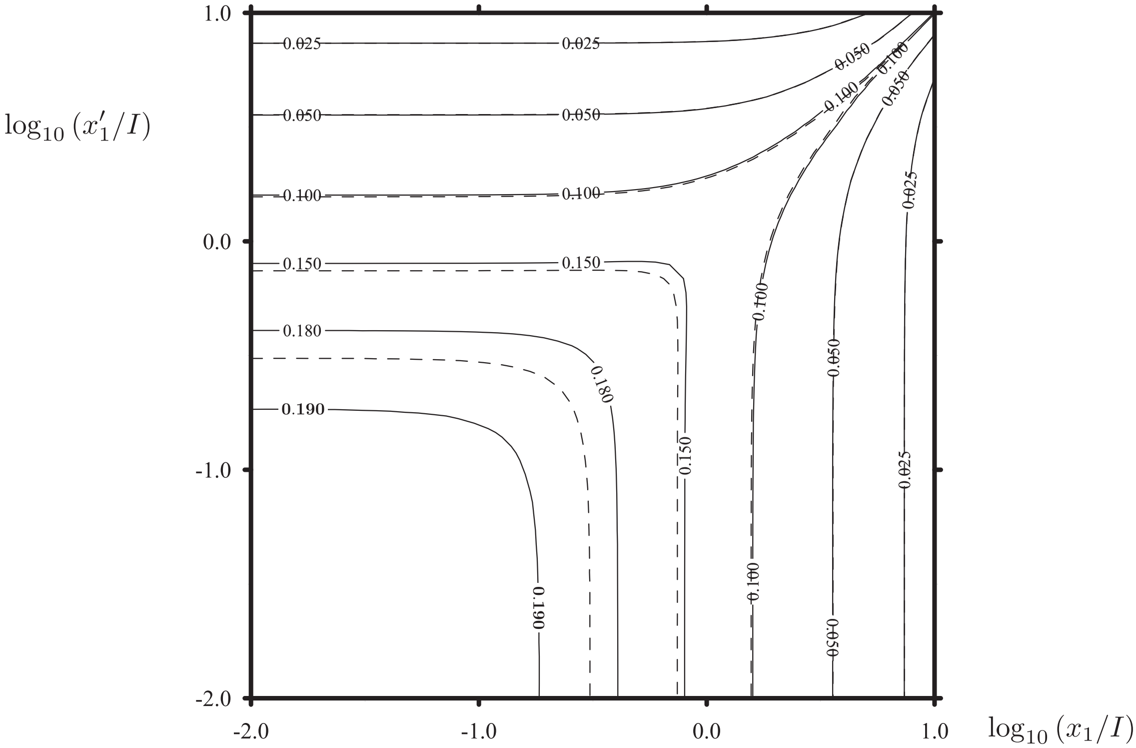

Fig. 2. Contour levels of the mean Green function G for $x_h = I$ for exponential (continuous line) and Gaussian (dashed line) autocorrelation ρ. Other parameters: $x_h = I$ and $\sigma^2 = 0.5$.

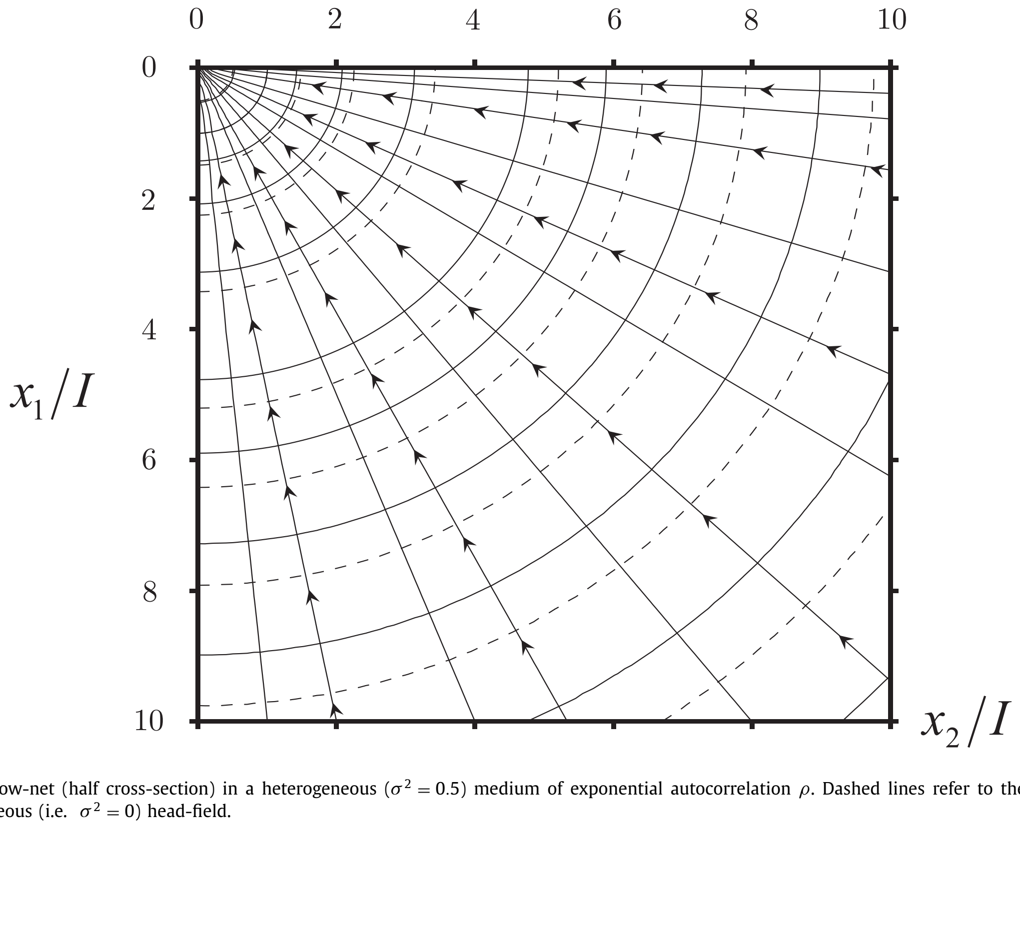

Fig. 3. The flow-net (half cross-section) in a heterogeneous ($\sigma^2 = 0.5$) medium of exponential autocorrelation ρ. Dashed lines refer to the iso-values of the homogeneous (i.e. $\sigma^2 = 0$) head-field.

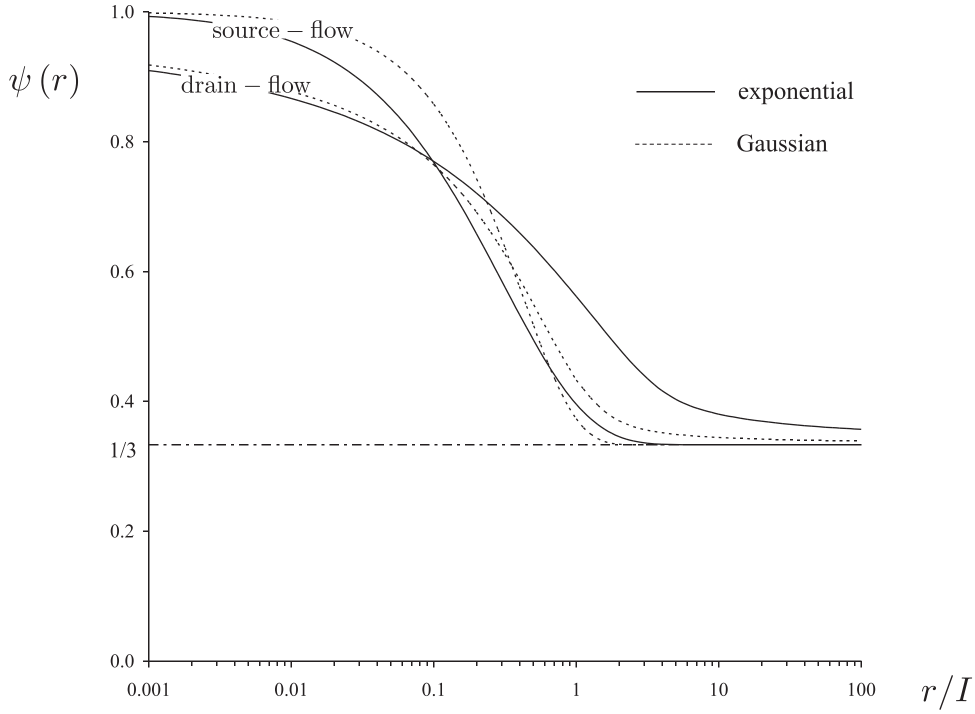

Fig. 4. The σ^2-order correction ψ to the mean Green function for exponential (continuous lines) and Gaussian (dashed lines) autocorrelation as function of the scaled distance r/I. The same function is depicted for a source flow.

In (18) and (19), $\mathrm{K}_\nu(x)$, $\mathrm{L}_\nu(x)$ and $\mathrm{W}_{a,b}(x)$ represent the modified Bessel, Struve and Whittaker functions, respectively. In the Fig. 3 we have depicted the flow-net in the vertical cross section. To emphasize the distortion-effect due to the heterogeneity upon the head-field, in the same figure we have also represented the homogeneous head distribution ($\varepsilon \equiv 0$). Similarly to [17] and [25], we represent the mean head as $\langle h(r)\rangle = \Psi(r)h_0(r)$, where we have set $\Psi(r) = 1 + \sigma^2\,\psi(r)$. In a different manner, the mean head is expressed as a product between h_0, and a characteristic function Ψ which "modifies" the homogeneous head h_0 according to the medium's heterogeneity. The normalized σ^2-correction $\psi(r) = \dfrac{\langle h_2(r)\rangle}{h_0(r)}$ results from (17) as

$$\psi(r) = \frac{1}{3}\left[1 - \frac{\omega(r)}{\ln r}\right]. \tag{20}$$

In particular, the expression (20) together with (18) and (19), permits one to derive the following asymptotics:

$$\psi(r) = 1 + \mathcal{O}\left(\frac{1}{\ln \bar{r}}\right) \quad (\bar{r} \ll 1), \qquad \psi(r) = \frac{1}{3} + \mathcal{O}\left(\frac{1}{\bar{r}}\right) \qquad (\bar{r} \gg 1). \tag{21}$$

Thus, close to the drain one has $\psi(0) = 1$ [in agreement with 17], whereas at large distances it yields: $\psi(\infty) = 1/3$. Note that this last result coincides with that obtained by Severino et al. [22] in the case of a Dirichlet condition at the source. This implies that, the type of boundary condition does not impact in the far field. Furthermore, close and far from the drain the flow behavior is not influenced by the shape of the correlation function. The function ψ is depicted in the Fig. 4 as function of the normalized radial distance r/I from the drain. Generally, $\psi(r)$ results monotonic decreasing approaching to 1/3 at large distances. In particular, the rate of getting such an asymptotic is higher in the case of Gaussian autocorrelation. For comparison purposes in the Fig. 4 we have also represented (blue face) the second order correction $\psi(r)$ due to a point-like source (which can be assimilated to the case of a very short drain) of given strength [see Eqs. (29) and (30) in 17]. It is seen that for $0 \leq r/I \leq 0.1$ the correction ψ to the mean Green function is more persistent for a short drain (blue line) than that pertaining to a long one (black line). As a consequence, within such a range the flow is more sensitive to the heterogeneity for a short drain. The situation is completely reversed for $r/I > 0.1$.

Computation of the equivalent conductivity

The non-uniformity of the mean flow defies in general the possibility to regard the effective conductivity as a medium's property [26]. More precisely, although effective properties can be derived at the σ^2-order of approximation for flows

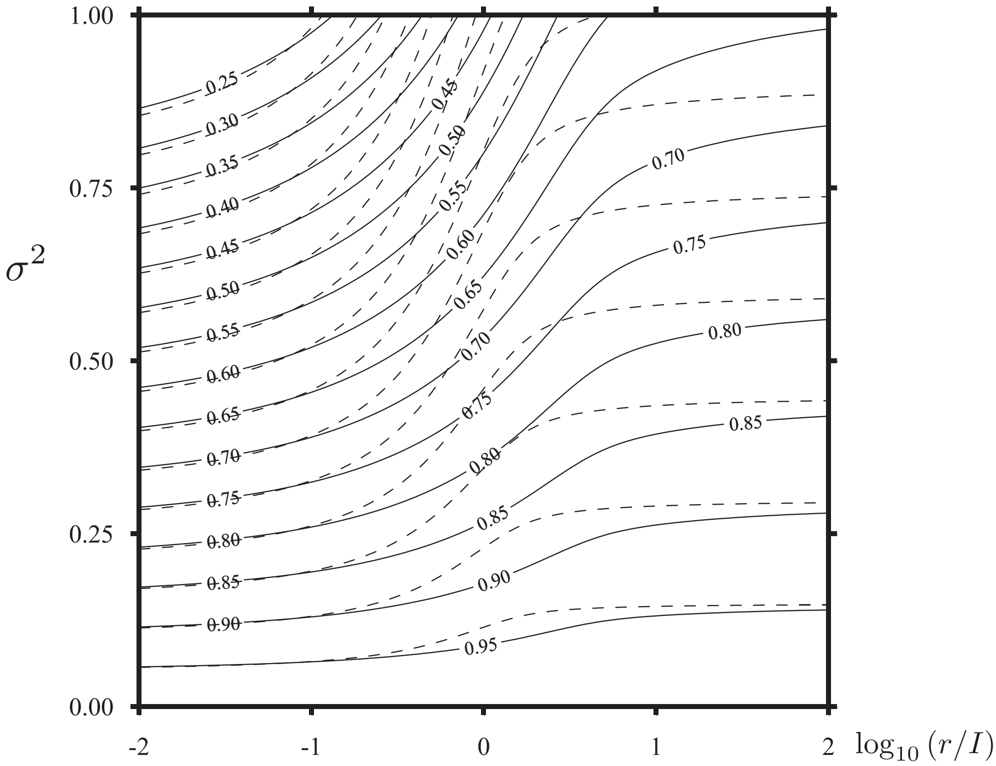

Fig. 5. Sensitivity of the normalized equivalent conductivity κ to the variance σ^2 and the scaled distance r/I. Continuous and dashed lines refer to exponential and Gaussian ρ, respectively.

generated by any source [see, e.g. 20], they nevertheless result function of quantities (such as the head gradient) that can not be measured in the field. For this reason, we introduce the concept of equivalent conductivity introduced by Matheron [27]. The equivalent conductivity $K^{eq}(r)$ is defined as the one of a fictitious homogeneous medium which conveys the same discharge Q_w as the actual, heterogeneous, formation, i.e.

$$\kappa(r) = \frac{K^{eq}(r)}{K_H} = \frac{h_0(r)}{\langle h(r) \rangle} = \Psi^{-1}(r) \simeq 1 - \sigma^2 \psi(r). \tag{22}$$

The advantage of this definition is that it expresses K^{eq} in terms of quantities which are measurable in the field. Instead, the drawback of this definition is that K^{eq} is not a medium property, but rather it results position-dependent. As a consequence, $K^{eq}(r)$ depends on the particular problem at stake, and therefore it cannot be used for other configurations.

In the Fig. 5 we have plotted the contour levels for both the exponential (continuous line), and the Gaussian (dashed line) autocorrelation. At small and large distances κ depends only upon the variance, and in particular one has: $\kappa(0) \le \kappa(r) \le \kappa(\infty)$. In a different manner, one can say that in these two extreme cases, the equivalent conductivity is a medium's property. In the intermediate regimes, the contour values are increasing with the distance r (given the variance σ^2).

We would like to emphasize that the present study strictly relies on a small-perturbation analysis, and therefore it is expected to be applicable whenever σ^2 is sufficiently small. However, it has been shown [28,29] that the range of applicability of the small perturbation approach is broader. In fact, the ensemble average procedure (that *de facto* is an expectation over many single realizations) induces a mutual cancellation of the errors due to the linearization procedure.

Summary and concluding remarks

The properties of head fields in porous media depend to a great extent on the flow domain configuration, and the formation's heterogeneity. In the past, many analytical (and semi-analytical) solutions of the steady flow equations have been derived for various boundary conditions in homogeneous aquifers [an extensive survey is provided by Bruggeman 24]. Later, the effect of the spatial variability of the hydraulic conductivity K on the head distribution has been intensively studied for flows uniform in the mean [5]. Instead, very few studies have dealt with non uniform mean flows, like those occurring in radial-type configurations [see, e.g. 17,30]. In addition, to our knowledge there are no analytical studies dealing with the similar problem as generated by a drain.

In the present paper steady flow toward a drain has been considered. Due to the linearity of the governing equations, we have focused on the derivation of the fundamental solution G (mean Green function) for the mean head in weakly heterogeneous porous formations (i.e. a solution which is accurate at the first order in the variance σ^2). Unlike the Green function valid for homogeneous media, here G depends on the medium statistical structure, as well. Closed-form solutions for G have been obtained for exponential and Gaussian correlations of isotropic structure.

We have then investigated the steady flow toward a drain by computing the mean head field $\langle h\rangle$. The main result is the general representation (16) that enables one to quantify the portion of the flow domain Ω which is more affected by the medium's heterogeneity. In view of its application to real world situations, we have then focused on the computation of the equivalent conductivity K_{eq} in order to cast this complex problem within the stand point of the theory of composites.

To conclude, besides the application to drains, the present study provides the way to compute the head fluctuation [by retaining the first order approximation in the perturbation expansion, similarly to 31] which is the prerequisite to investigate the dispersion mechanisms of agrochemicals in soils under radial-type flow configurations along the lines of [32], and [33]. These topics are already part of ongoing research projects.

Acknowledgments

The present study was developed within the GNCS (Gruppo Nazionale Calcolo Scientifico – INdAM) framework. The first author acknowledges the valuable assistance during the literature review provided by Giovanna Ameno (*Department of* Agricultural Sciences, University of Naples – Federico II, Italy).

Appendix A. Computation of the function $\omega \equiv \omega(r)$

The evaluation of the σ^2-order correction to the mean head is reduced to the computation of the function ω appearing into (17), with

$$\Lambda(x) = \frac{1}{\sqrt{x}} + \frac{2}{\sqrt{x}}\left(1 + \frac{\sqrt{x}}{4} - \frac{x}{4}\right)\exp\left(-\sqrt{x}\right) + \left(2 - \frac{x}{3}\right)\mathrm{Ei}\left(-\sqrt{x}\right) \tag{A1}$$

for exponential, and

$$\Lambda(x) = \frac{1}{\sqrt{x}} + \frac{2}{\sqrt{x}}\left(1 + \frac{\pi}{4}x\right)\exp\left(-\frac{\pi}{4}x\right) - \frac{\pi}{4}(6 + \pi x)\mathrm{erfc}\left(\frac{\sqrt{\pi x}}{2}\right) \tag{A2}$$

for Gaussian autocorrelation, respectively. It is convenient to preliminarily decompose the integral appearing into (17) as: $\int_0^\infty d\xi\, \Lambda\left(\xi^2 + r^2\right) = I_1(r) + I_2(r) + I_3(r)$ being the various $I_i(r)$ defined via the addends in (A1) and (A2).

Exponential autocorrelation

In this case it is easy to show from the first term on the rhs of (A1) that

$$I_1(r) = \int_0^\infty \frac{d\xi}{\sqrt{\xi^2 + r^2}} = -\ln r. \tag{A3}$$

The integral I_2 stems from the second term on the rhs of (A1) as

$$I_2(r) = 2\int_0^\infty \frac{d\xi}{\sqrt{\xi^2 + r^2}}\left(1 + \frac{\sqrt{\xi^2 + r^2}}{4} - \frac{\xi^2 + r^2}{4}\right)\exp\left(-\sqrt{\xi^2 + r^2}\right). \tag{A4}$$

In order to evaluate (A4) we introduce the new variable $u = \sinh^{-1}(\xi/r)$ so that

$$I_2(r) = \frac{1}{2}\int_0^\infty du[4 + r\cosh u(1 - r\cosh u)]\exp(-r\cosh u) = \left(2 - \frac{r^2}{2}\right)\mathrm{K}_0(r) \tag{A5}$$

[34]. Finally, $I_3(r)$ is (third term on the rhs of (A1))

$$\begin{aligned} I_3(r) &= \int_0^\infty d\xi\left(2 - \frac{\xi^2 + r^2}{3}\right)\mathrm{Ei}\left(-\sqrt{\xi^2 + r^2}\right) \\ &= \int_0^\infty \frac{d\xi\, \xi^2}{\xi^2 + r^2}\left(\frac{\xi^2}{9} + \frac{r^2}{3} - 2\right)\exp\left(-\sqrt{\xi^2 + r^2}\right), \end{aligned} \tag{A6}$$

being the second integral obtained after integrating by parts. The last quadrature into (A6) is performed similarly to the previous case, i.e.

$$I_3(r) = \frac{r^2}{9}\mathrm{K}_2(r) + \frac{r}{9}\left(r^2 - 9\right)\left\{2[\mathrm{K}_1(r) + r\mathrm{K}_0(r)] + \pi r\left[\mathrm{K}_0(r)\mathrm{L}_1(r) + \mathrm{K}_1(r)\mathrm{L}_0(r) - \frac{1}{r}\right]\right\}. \tag{A7}$$

Hence, summing the second of (A5) with (A6) and (A7) leads to (18).

Gaussian autocorrelation

The first integral $I_1(r)$ coincides with (A3). The integral $I_2(r)$ comes from the integration of the second term of on the rhs of (A2), i.e.

$$I_2(r) = 2\int_0^\infty \frac{d\xi}{\sqrt{\xi^2+r^2}}\left[1+\frac{\pi}{4}\left(\xi^2+r^2\right)\right]\exp\left[-\frac{\pi}{4}\left(\xi^2+r^2\right)\right]. \tag{A8}$$

By performing the same change of variable as before, one has

$$I_2(r) = \exp\left(-\frac{\pi}{8}r^2\right)\left[\frac{\pi}{8}r^2\,\mathrm{K}_1\left(\frac{\pi}{8}r^2\right)+\left(1+\frac{\pi}{8}r^2\right)\mathrm{K}_0\left(\frac{\pi}{8}r^2\right)\right] \tag{A9}$$

[34]. Last, $I_3(r)$ is obtained by integrating the third term on the rhs of (A2), i.e.

$$\begin{aligned} I_3(r) &= -\frac{\pi}{4}\int_0^\infty d\xi\left[6+\pi\left(\xi^2+r^2\right)\right]\mathrm{erfc}\left[\frac{1}{2}\sqrt{\pi\left(\xi^2+r^2\right)}\right] \\ &= -\frac{\pi}{4}\int_0^\infty \frac{d\xi\,\xi^2}{\sqrt{\xi^2+r^2}}\left[6+\pi\left(r^2+\frac{\xi^2}{3}\right)\right]\exp\left[-\frac{\pi}{4}\left(\xi^2+r^2\right)\right], \end{aligned} \tag{A10}$$

where the last derivation has been achieved by integrating by parts. By carrying out the last quadrature gives

$$I_3(r) = \frac{\pi}{4}r\exp\left(-\frac{\pi}{8}r^2\right)\left\{\frac{r}{4}\left(6+\pi r^2\right)\left[\mathrm{K}_0\left(\frac{\pi}{8}r^2\right)-\mathrm{K}_1\left(\frac{\pi}{8}r^2\right)\right]-\mathrm{W}_{-1,1}\left(\frac{\pi}{4}r^2\right)\right\}. \tag{A11}$$

Summing the three contributions $I_i(r)$ yields (19).

Appendix B. List of symbols

Δ	-	Drain's length
$\mathbf{e} \equiv (e_1, e_2)^\top$	-	Unit vector
$\varepsilon(\boldsymbol{x})$	-	Residual of $1 - K(\boldsymbol{x})/\langle K\rangle$
$G_\infty^{(0)}(x)$	-	Homogeneous Green function pertaining to the free space $\mathbb{R}^3$
$G(\boldsymbol{x}, \boldsymbol{x}')$	-	Mean Green function pertaining to the half space in $\mathbb{R}^3$
$G_\infty^{(2)}(\boldsymbol{x})$	-	Second order correction to the mean Green function in $\mathbb{R}^3$
$h(\boldsymbol{x})$	-	Hydraulic head
$h_2(\boldsymbol{x})$	-	σ^2 order correction to h
$I \equiv \int_0^\infty \mathrm{d}x\,\rho(x)$	-	Integral scale of heterogeneity
$\mathrm{L}_\nu(x)$	-	ν-order Struve function
$\Lambda(x)$	-	Characteristic function (15)
$K(\boldsymbol{x})$	-	Hydraulic conductivity
$\langle K\rangle$	-	Arithmetic mean of K
K_H	-	Harmonic mean of K
$K^{\mathrm{eq}}(r)$	-	Equivalent conductivity
$\mathrm{K}_\nu(x)$	-	Modified ν-order Bessel function
$\kappa(r)$	-	Normalized equivalent conductivity
Ω	-	Flow domain
$\Psi(\boldsymbol{x})$	-	Characteristic heterogeneity function
$\psi(\boldsymbol{x})$	-	Normalized second order correction to the Green Function
$\rho(\boldsymbol{x})$	-	Autocorrelation function of $\varepsilon(\boldsymbol{x})$
Q_w	-	Volumetric (per unit length) discharge at the drain
$\tilde{Q}_w$	-	Q_w divided by K_H
$\mathbf{q} \equiv (q_1, q_2, q_3)^\top$	-	Flux
$r = \sqrt{x_1^2 + x_2^2}$	-	Radial distance from the drain
r_d	-	Drain radius
σ^2	-	Variance of $\varepsilon(\boldsymbol{x})$
σ_K^2	-	Variance of $K(\boldsymbol{x})$
$\mathrm{W}_{a,b}(x)$	-	Whittaker function
$\boldsymbol{x} \equiv (x_1, x_2, x_3)$	-	Position in Ω
$a \equiv \lvert\boldsymbol{a}\rvert = \sqrt{a_1^2 + a_2^2 + a_3^2}$	-	Magnitude of the vector $\boldsymbol{a}$
$\langle\rangle$	-	Ensemble average operator
$\cdot$	-	"Dot" product
MCs	-	Monte Carlo simulations
RSF	-	Random space function

References

[1] G. Severino, M. Scarfato, A. Comegna, Stochastic analysis of unsaturated steady flows above the water table, Water Resour. Res. 53 (8) (2017) 6687–6708, doi:10.1002/2017WR020554.
[2] L. Gurovich, P. Oyarce, Modeling agricultural drainage hydraulic nets, Irrig. Drain Syst. Eng. 4 (2015) 149–158, doi:10.4172/2168-9768.1000149.
[3] G. De Schepper, R. Therrien, J.C. Refsgaard, A.L. Hansen, Simulating coupled surface and subsurface water flow in a tile-drained agricultural catchment, J. Hydrol. 521 (2015) 374–388, doi:10.1016/j.jhydrol.2014.12.035.

[4] Y. Rubin, Applied Stochastic Hydrogeology, Oxford University Press, 2003.
[5] G. Dagan, Flow and Transport in Porous Formation, Springer-Verlag, 1989.
[6] L.W. Gelhar, Stochastic Subsurface Hydrology, Prentice Hall, 1993.
[7] C. Fallico, S. De Bartolo, M. Veltri, G. Severino, On the dependence of the saturated hydraulic conductivity upon the effective porosity through a power law model at different scales, Hydrol. Process. 30 (13) (2016) 2366–2372, doi:10.1002/hyp.10798.
[8] C. Fallico, M. Ianchello, S. De Bartolo, G. Severino, Spatial dependence of the hydraulic conductivity in a well-type configuration at the mesoscale, Hydrol. Process. 32 (4) (2018) 590–595, doi:10.1002/hyp.11422.
[9] G. Severino, A. Santini, V.M. Monetti, Modelling water flow and solute transport in heterogeneous unsaturated porous media, in: Advances in Modeling Agricultural Systems, Springer, US, 2009, pp. 361–383, doi:10.1007/978-0-387-75181-8_17.
[10] M. Sahimi, Heterogeneous Materials I: Linear transport and optical properties, 22, Springer Science & Business Media, 2003.
[11] T.C. Choy, Effective Medium Theory: Principles and Applications, Oxford University Press, 2015.
[12] I. Jankovic, A. Fiori, G. Dagan, Flow and transport in highly heterogeneous formations: 3. Numerical simulations and comparison with theoretical results, Water Resour. Res. 39 (9) (2003) SBH16–1, doi:10.1029/2002WR001721.
[13] D. Zhang, Stochastic Methods for Flow in Porous Media, Academic Press, 2002.
[14] M. Di Dato, A. Fiori, F.P.J. de Barros, A. Bellin, Radial solute transport in highly heterogeneous aquifers: modeling and experimental comparison, Water Resour. Res. 53 (7) (2017) 5725–5741, doi:10.1002/2016WR020039.
[15] A. Zech, C. D'Angelo, S. Attinger, A. Fiori, Revisitation of the dipole tracer test for heterogeneous porous formations, Adv. Water Resour. 115 (2018) 198–206, doi:10.1016/j.advwatres.2018.03.006.
[16] G. Severino, S. Leveque, G. Toraldo, Uncertainty quantification of unsteady source flows in heterogeneous porous media, J. Fluid Mech. 870 (2019) 5–26, doi:10.1017/jfm.2019.203.
[17] P. Indelman, Steady-state source flow in heterogeneous porous media, Transp. Porous Med. 45 (1) (2001) 105–127, doi:10.1023/A:1011814418142.
[18] G. Dagan, A note on packer, slug, and recovery tests in unconfined aquifers, Water Resour. Res. 14 (5) (1978) 929–934, doi:10.1029/WR014i005p00929.
[19] G. Severino, Stochastic analysis of well-type flows in randomly heterogeneous porous formations, Water Resour. Res. 47 (3) (2011), doi:10.1029/2010WR009840.
[20] P. Indelman, B. Abramovich, Nonlocal properties of nonuniform averaged flows in heterogeneous media, Water Resour. Res. 30 (12) (1994) 3385–3393, doi:10.1029/94WR01782.
[21] A. Guadagnini, M. Riva, S.P. Neuman, Three-dimensional steady state flow to a well in a randomly heterogeneous bounded aquifer, Water Resour. Res. 39 (3) (2003) 1048, doi:10.1029/2002WR001443.
[22] G. Severino, A. Santini, A. Sommella, Steady flows driven by sources of random strength in heterogeneous aquifers with application to partially penetrating wells, Stoch. Environ. Res. Risk Assess. 22 (4) (2008) 567–582, doi:10.1007/s00477-007-0175-5.
[23] C.C. Mei, Mathematical Analysis in Engineering: How to Use the Basic Tools, Cambridge University Press, 1997.
[24] G.A. Bruggeman, Analytical Solutions of Geohydrological Problems, Elsevier, 1999.
[25] G. Severino, Macrodispersion by point-like source flows in randomly heterogeneous porous media, Transp. Porous Med. 89 (1) (2011) 121–134, doi:10.1007/s11242-011-9758-1.
[26] G. Severino, A. Santini, On the effective hydraulic conductivity in mean vertical unsaturated steady flows, Adv. Water Resour. 28 (2005) 964–974, doi:10.1016/j.advwatres.2005.03.003.
[27] G. Matheron, Elements Pour une Theorie des Milieux Poreux, Masson, 1967.
[28] I. Jankovic, A. Fiori, G. Dagan, Effective conductivity of an isotropic heterogeneous medium of lognormal conductivity distribution, Multiscale Model. Simul. 1 (1) (2003) 40–56, doi:10.1137/S1540345902409633.
[29] G. Severino, Effective conductivity in steady well-type flows through porous formations, Stoch. Environ. Res. Risk Assess. 33 (3) (2019) 827–835, doi:10.1007/s00477-018-1639-5.
[30] D.M. Tartakovsky, S.P. Neuman, Transient effective hydraulic conductivities under slowly and rapidly varying mean gradients in bounded three-dimensional random media, Water Resour. Res. 34 (1) (1998) 21–32, doi:10.1029/97WR01965.
[31] A. Fiori, P. Indelman, G. Dagan, Correlation structure of flow variables for steady flow toward a well with application to highly anisotropic heterogeneous formations, Water Resour. Res. 34 (4) (1998) 699–708, doi:10.1029/97WR02491.
[32] P. Indelman, Y. Rubin, Solute transport in nonstationary velocity fields, Water Resour. Res. 32 (5) (1996) 1259–1267, doi:10.1029/95WR03238.
[33] P. Indelman, G. Dagan, Solute transport in divergent radial flow through heterogeneous porous media, J. Fluid Mech. 384 (1999) 159–182, doi:10.1017/S0022112098004078.
[34] I.S. Gradshteyn, I.M. Ryzhik, Table of Integrals, Series, and Products, Academic Press, 2014.